Proceedings World Geothermal Congress 2020+1
Reykjavik, Iceland, April - October 2021

# A Comparison of the Greywacke Basement in Kawerau and Rotokawa Geothermal Fields in Taupo Volcanic Zone, New Zealand

Aimee A. Calibugan[1], Isabelle Chambefort[2] and Farrell Siega[1]

[1]Mercury NZ Ltd, 283 Vaughan Road, Rotorua 3010, New Zealand

[2]GNS Science, Wairakei Research Centre, 114 Karetoto Road, Taupo 3384, New Zealand

Aimee.Calibugan@mercury.co.nz

**Keywords:** Kawerau, Rotokawa, greywacke basement, Torlesse composite terrane, Waipapa composite terrane, Taupo Volcanic Zone

## ABSTRACT

This paper aims to present the results of the petrological and mineralogical analyses conducted on selected greywacke basement samples from the Kawerau and Rotokawa Geothermal Fields. These two fields are both found within the Taupo Volcanic Zone (TVZ), as with most of the active geothermal fields in New Zealand. The Kawerau Geothermal Field lies near the northeast boundary of TVZ while the Rotokawa Geothermal Field is situated close to the southeast boundary. The study is conducted to determine if there are distinct differences in the petrography and mineralogy in the greywackes that may provide insight on the observed difference in injection well performance in the two fields.

Results of petrographic assessments indicate that the Kawerau greywacke is characterized by well-sorted, clast-supported metasandstone to siltstone with common volcanic clasts of intermediate composition whereas the Rotokawa greywackes vary from matrix-dominated, well-sorted metasandstone to argillite. Overall, the samples from Rotokawa can be classified as part of the Torlesse Composite Terrane (Kaweka Terrane) while samples from Kawerau can be grouped under the Waipapa Composite Terrane (Morrinsville Facies). A variation in the mineralogy of the two greywackes is also observed with the Rotokawa greywacke having rare calcite / chlorite while Kawerau greywacke has abundant calcite / chlorite. The abundance of these two minerals in the Kawerau greywacke is possibly influencing the rock reactivity to acid-dosed brine resulting to buffering of the injection fluid pH. This may potentially help explain the observed difference in injection well performance between the two fields, however other contributing factors cannot be discounted (e.g. temperature differences).

## 1. INTRODUCTION

New Zealand high enthalpy geothermal fields are located within the Taupo Volcanic Zone (TVZ; except Ngawha in the North) which lies in the central part of the North Island of New Zealand. The TVZ is a rifting arc associated with the oblique subduction of the Pacific plate beneath New Zealand (Wood et al., 2001). The volcanic region is flanked and underlain by basement rocks of the Torlesse and Waipapa composite terranes (Adams et al., 2009; Mortimer et al., 2014; Price, et al., 2015). Figure 1 shows the location of Rotokawa and Kawerau Geothermal Fields in the TVZ.

The Rotokawa Geothermal Field extends over an area of ~28 km$^2$ based on shallow resistivity mapping (Risk, 2000) and has an installed capacity of 174 MWe capacity (Hernandez et al., 2015). The field is located near the southeastern boundary of the TVZ. Exploratory drilling at Rotokawa was carried out between 1965 to 1986 that confirmed the presence of a high-temperature (>300˚C) resource (Cole and Legmann, 1998; White and Chambefort, 2016). Drilling encountered the top of the greywacke basement in the southeast at depths between -1612 mRL and -1929 mRL (metres relative to sea level) and this is down-faulted towards the central part of the field and was intersected at -2720 mRL. A 3D model of the top of the basement greywacke at Rotokawa is shown in Figure 1. The greywacke basement in the southeast is hosting bulk of the brine and condensate injection for the Rotokawa field.

The Kawerau Geothermal Field, as defined by low resistivity signature, occupies an area of 35 km$^2$ (Askari et al., 2015) and it is a multi-tapper field with a total combined installed capacity of 173 MWe (Bloomer, 2015; NZGA, 2019). The field lies near the northeastern tip of the TVZ. Drilling in Kawerau began in 1951 (White and Chambefort, 2016) and to date more than 70 wells have been drilled up to 3 km depth (Milicich et al., 2015). A 3D model of the top of the basement greywacke at Kawerau is shown in Figure 1. The greywacke is inferred to be down-faulted to the northwest and drilled from −667 mRL in the southeast, on the upfaulted eastern margin of the Whakatane Graben, to −1426 mRL on the northwest margin of the field (Milicich et al., 2015). Both production and injection at Kawerau are hosted by the greywacke basement.

This paper presents a petrographic review of the greywacke basement reservoir rocks from Rotokawa and Kawerau Geothermal Fields to elucidate the role of greywacke on silica scaling in the reservoir upon injection. There has been no previous comparative study conducted on the basement rocks of the two fields, although Wood et al. (2001) did a study on the Ohaaki and Kawerau basement rocks and reported a significant variation in the mineralogical and permeable properties between the two fields.

## 2. GEOTHERMAL SILICA MANAGEMENT VIA ACID-DOSING

Silica scaling remains to be one of the key challenges encountered commonly in geothermal operation. Addison et al. (2015) discussed in detail some of the options to minimize scaling risk other than injecting brine with low silica saturation index (SSI) including: 1) avoidance of reinjecting geothermal brine; 2) use of silica removal equipment; 3) pH modification using acid to lower pH; 4) caustic dosing to increase pH; 5) use of anti-scalant; and 6) dilution with steam condensate.

Both the Rotokawa field and the Kawerau Geothermal Limited (KGL) plant, one of the tappers of the Kawerau reservoir, utilize pH modification via addition of sulfuric acid and/or steam condensate to control silica scaling (Addison et al., 2015). The objective of acid-dosing is to lower the pH of the injected brine to retard the silica polymerization process until the brine is injected well into the formation (i.e. away from the wellbore).

However, there are relative differences in injection well performance observed in these fields. This paper will look into the petrography and mineralogy of the injection host rocks (greywackes) to understand if rock characteristic is a factor for this.

## 3. WAIPAPA AND TORLESSE COMPOSITE TERRANES

Mortimer et al. (2014) introduced a new high-level stratigraphic framework for all rocks and unconsolidated sediments in New Zealand. The updated framework retained the mapping for all Cambrian–Early Cretaceous basement rocks into the Eastern Province and Western Province. The Eastern Province includes the Waipapa and Torlesse composite terranes (Figure 2). The boundary between the Waipapa and Torlesse composite terranes is not well delineated within the TVZ as there are covered by Quaternary rocks (Price et al. (2015). The metasedimentary terrane beneath the Taupo Volcanic Zone is composed of two groups: the Waipapa composite terrane in the northeast and the Torlesse (Kaweka and Pahau) in the southwest (Figure 2; Adams et al., 2009; Mortimer et al., 2014; Price, et al., 2015).

Beetham and Watters (1985) reported that petrographic, modal, and chemical data indicated that the Torlesse rocks are more siliceous and contain abundant granitic debris whereas the Waipapa terrane rocks are considerably less siliceous, and typical sandstones have a high content of intermediate volcanic clasts. In 2001, Wood et al. compared the greywackes at Ohaaki and Kawerau and concluded that the greywackes at Ohaaki are of "granite-rhyolite" provenance and have more interbedded argillite than the "andesite-dacite" derived Kawerau greywackes. The greywacke basement at Rotokawa is interpreted to be similar to the Ohaaki basement based on mineralogy and facies.

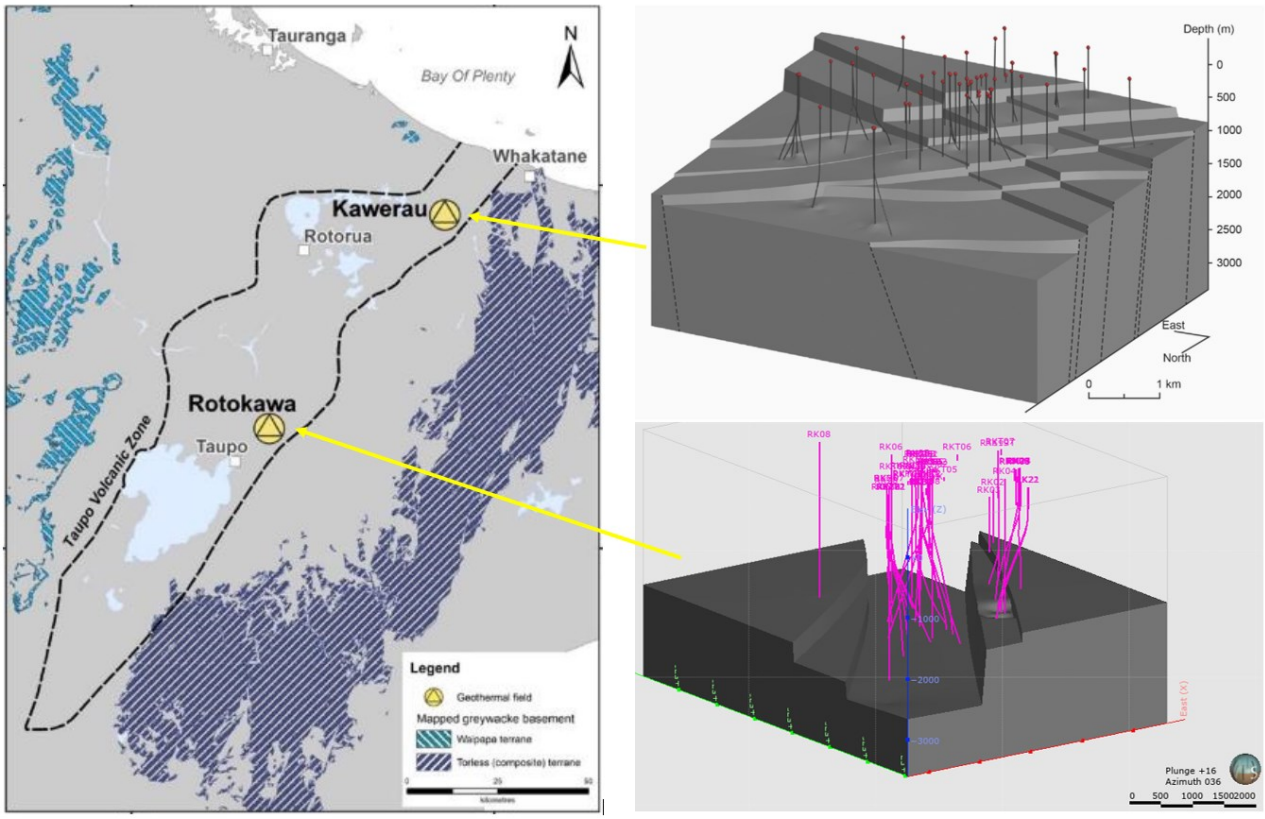


**Figure 1: Left: Location map of the Rotokawa and Kawerau Geothermal Fields in the TVZ. Right: 3D visualisation models of the top of the greywacke basement at Kawerau (Milicich et al., 2015) and Rotokawa (Milicich et al., 2019; 2020 this volume).**

Price et al. (2015) indicated that the samples from the Kaweka Terrane, which is part of the Torlesse Composite Terrane, tend to have higher $SiO_2$ and $Al_2O_3$, but lower $Fe_2O_3$ and MgO compared to Waipapa Terrane counterparts. They added that the Kaweka Terrane sandstones have $SiO_2$ abundances ranging from 68.6 to 74 wt%, whereas Waipapa sandstones have relatively lower $SiO_2$ contents (59.5–66.1 wt%). They also observed an overall negative correlation between $Al_2O_3$, total $Fe_2O_3$ and MgO contents with $SiO_2$ abundance, hence abundances of these major elements tend to be higher in the Waipapa Terrane samples relative to the Torlesse sample suite.

A summary of the main petrographic characteristics of the two basement terranes based on Wood et al. (2001) and Price et al. (2015) is shown in Table 1.

**Table 1: Main petrographic characteristics of the Torlesse and Waipapa basement terranes.**

| Terrane | Rock Descriptions | Accessory Minerals | Average $SiO_2$ content |
|---|---|---|---|
| Waipapa (Morrinsville Facies) | • Volcanic litharenites of andesitic-dacitic origin.<br>• Medium grained sandstone with subangular clasts, minor argillite.<br>• Clast supported and matrix poor. | 50% volcanics, abundant plagioclase, moderate quartz, minor K-Feldspar, biotite and muscovite | 59.5–66.1 wt% |
| Torlesse (Kaweka) | • Interbedded hard grey, medium to fine grained sandstone (greywacke) with (3%) argillite.<br>• Matrix supported. | Detrital quartz, plagioclase, minor K-feldspar, volcanics, biotite. Abundant (31%) clay-rich matrix | 68.6 to 74 wt% |

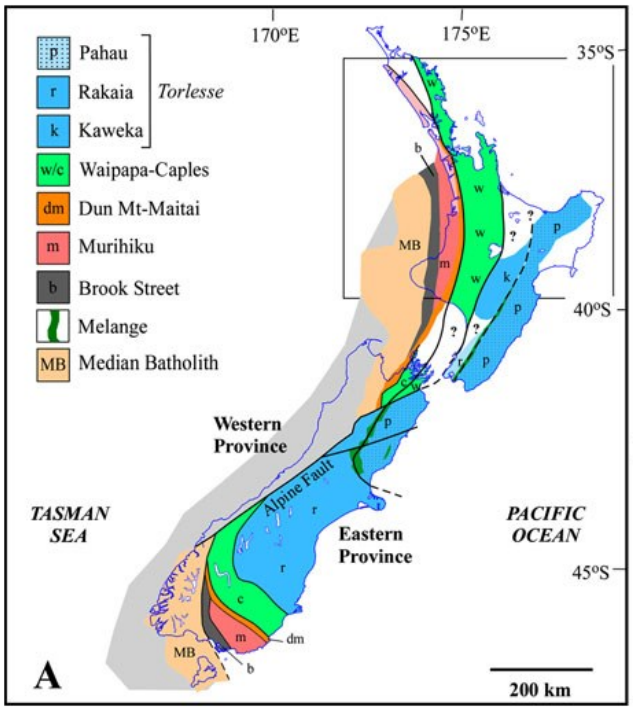


**Figure 2: Map of New Zealand North and South islands showing distribution of Torlesse and Waipapa terranes of the Eastern Province (Price et al., 2015).**

## 4. SAMPLE SELECTION AND METHOD

Figure 3 shows the sample location map for the Kawerau and Rotokawa greywackes used in the study. Samples were selected based on core accessibility, textures and as much as possible proximity to the main permeable zone of the wells. Six greywacke samples were collected from Rotokawa particularly from wells in the southeast portion of the field (Figure 3). Another six greywacke samples were obtained from the northern and northeastern injection areas of the Kawerau field (Figure 3). A total of twelve cutting and core samples were prepared into epoxy mounts and polished (Figure 4). Backscattered and energy dispersive X-Ray analyses were determined using a JEOL NEOSCOPE 6000plus Desktop Scanning Electron Microscope (SEM) at GNS Science Wairakei Research Centre, with an accelerating voltage of 10 kV and a high probe current of 20 nA in high vacuum set up.

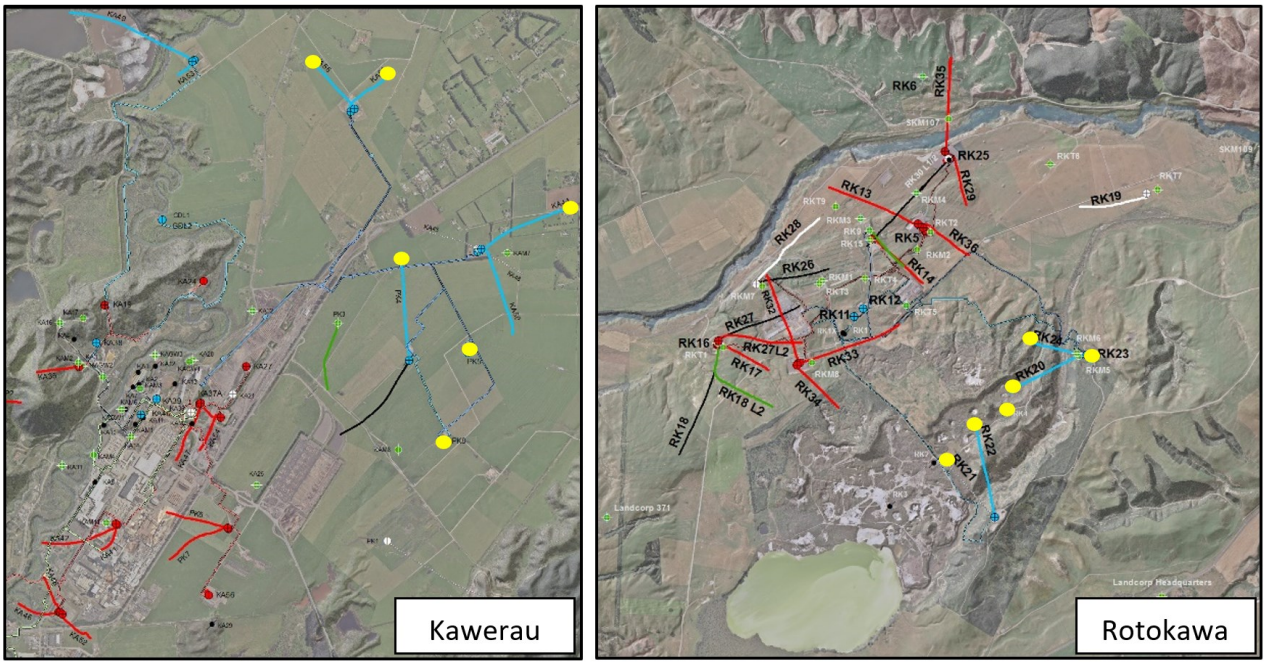


**Figure 3: Sample location map for Rotokawa and Kawerau greywackes used in the study (wells marked by yellow circles).**

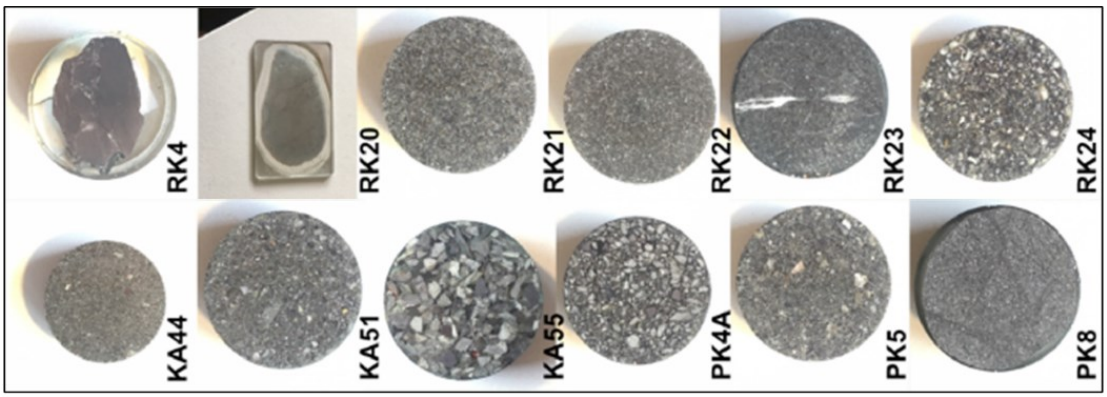


**Figure 4: Epoxy mounts of Rotokawa and Kawerau greywacke samples.**

## 5. RESULTS

### 5.1 Petrography

Figure 5 to Figure 8 **Error! Reference source not found.**illustrate the diverse characteristics of the Rotokawa greywackes which vary from matrix-dominated, well-sorted metasandstone to argillite. RK23 samples (2,448 mRF) consist of relatively well-sorted fine-grained siltstone to sandstone and shown in Figure 5 is a litharenitic texture with subangular clasts of quartz, plagioclase (overprinted by albite and adularia), titanite and perthitic-textured clasts, within an illite-rich matrix with minor chlorite. Drilled on the same pad with RK23, the RK24 (2,250 mRF) samples are characterized by well-sorted very fine-grained sandstone to mudstone/argillite. **Error! Reference source not found.** shows a matrix-supported siltstone with illite-altered matrix from RK24. Most of the grains have abundant silicification with minor albitisation and adularia replacement.

Slightly to the south of RK23 and RK24, both RK20 (2,600 mRF) and RK4 (2,394 mRF) have cores showing very fine-grained mudstone. Figure 7 shows a quartz-illite replaced mudstone with rare chlorite, epidote and sulfide from the RK20 core. In the same sample, a metamorphic vein with REE-bearing epidote, monazite, pyrite, chlorite and quartz was also observed. The rock is dominantly composed of quartz, albite and illite with rare adularia and chlorite.

Further south, RK21 (2,400 mRF) and RK22 (2,680 mRF) cuttings show very diverse fragments. Some of the RK22 cuttings have deformed sandstone indicating ductile deformation likely associated with the metamorphic event (Figure 8). In contrast, some of the RK21 cuttings, are strongly brecciated, deformed fragments suggestive of fault deformation.

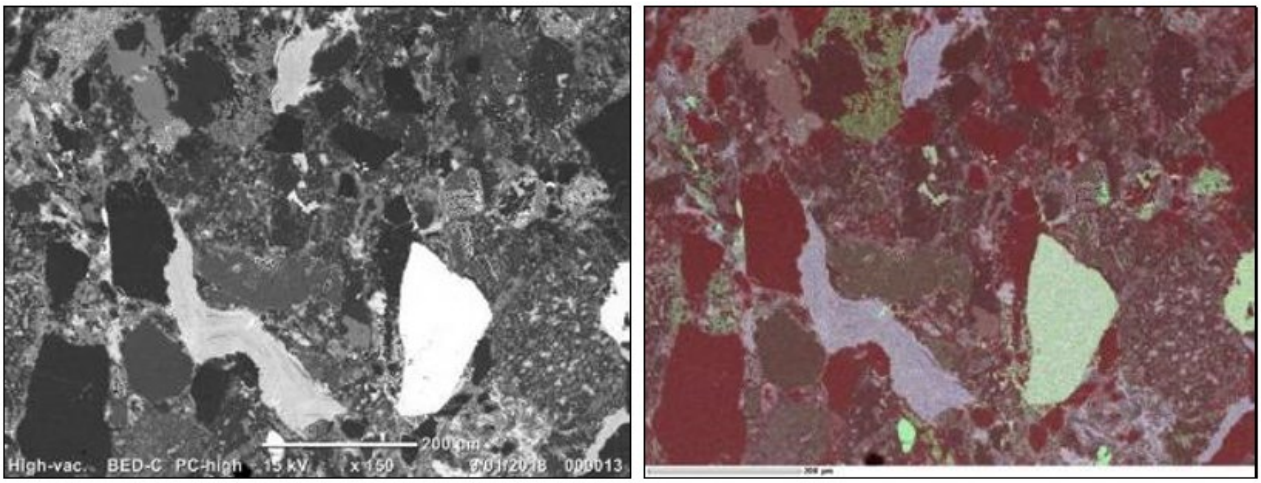


**Figure 5: RK23-2680 mRF (left) litharenite characterized by subangular clasts of quartz, plagioclase (overprinted by albite and adularia), titanite and perthitic-textured clasts, within an illite-rich matrix with minor chlorite. EDS chemical composite map (right) - red: $SiO_2$ (quartz, feldspar), blue: Mg (chlorite), green: Ca (titanite, calcite, plagioclase).**

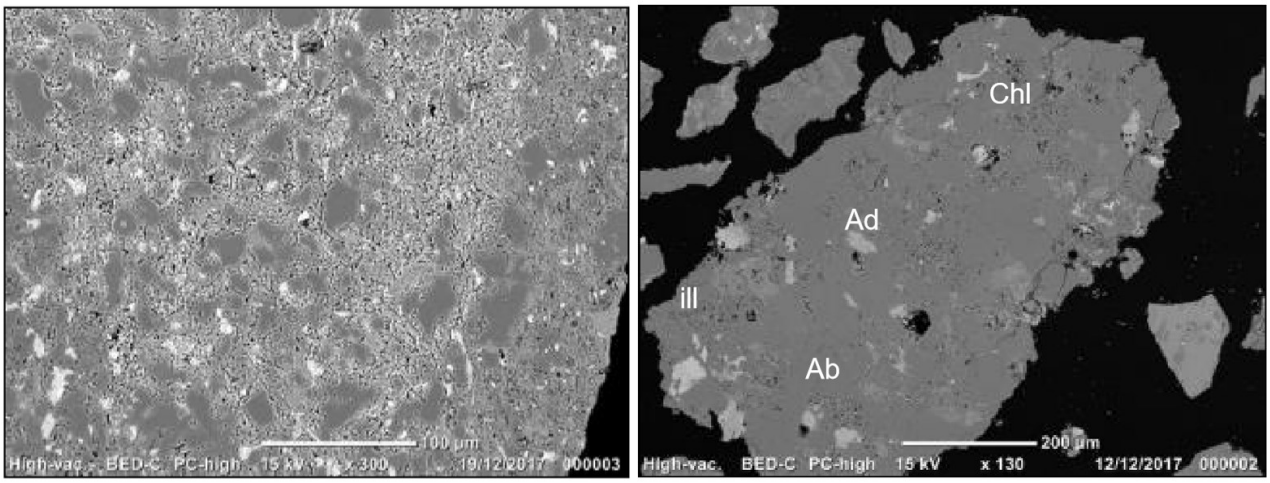


**Figure 6: RK24-2250 mRF (left) matrix-supported fine-grained siltstone with illite-altered matrix and small crystal of chlorite. Majority of the grains show abundant silicification with minor albitisation and adularia replacement. Right: Illite and albite altered plagioclase with small grained of adularia and chlorite.**

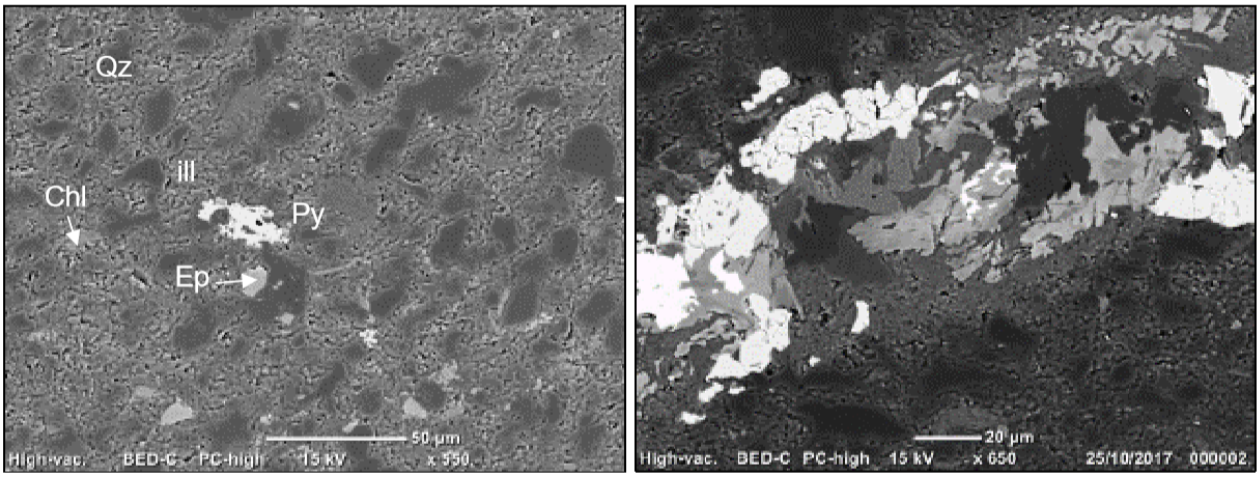


**Figure 7: RK20-2600 mRF (left) quartz-illite replaced mudstone with rare chlorite, epidote and sulfide. Metamorphic vein (right) with REE-bearing epidote, monazite, pyrite, chlorite and quartz. This rock is dominantly composed of quartz, albite and illite with rare adularia and chlorite.**

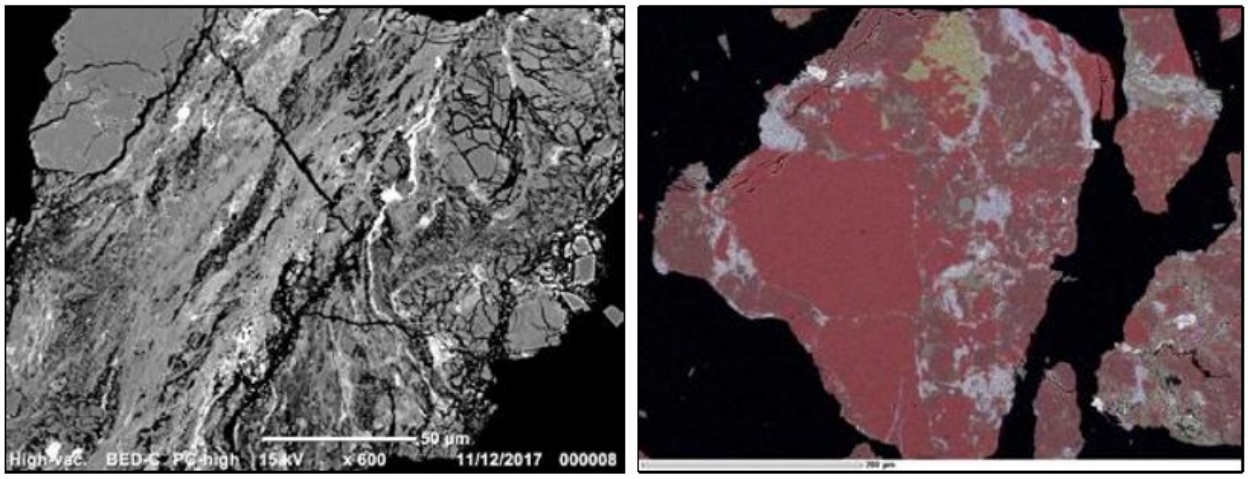


**Figure 8: RK22-2680 mRF. Left: Intensely chlorite + illite-altered, deformed sandstone showing ductile deformation likely associated with the metamorphic event. Rare pyrite occurs in the matrix (bright white wispy mineral). Plagioclase or K-felspar clasts are entirely albitised. Right: Fragment with a large quartz grain (red) surrounded by a fine matrix of chlorite and illite. Potassic alteration (adularia; yellow) is partially replacing the feldpar. EDS chemical composite map, red: $SiO_2$, blue: Mg (chlorite), green/yellow: K (adularia).**

Kawerau greywackes, in contrast, are generally well-sorted, clast-supported metasandstone to siltstone with common volcanic clasts of intermediate composition. Starting in the northern injection area, KA55 cuttings (1,580 mRF) show fine-grained siltstone to sandstone with fragments of primary quartz, plagioclase, altered to quartz, chlorite, illite epidote, albite with rare calcite and sulfide. The nearby KA51 (cuttings from 1,670 mRF) is characterized by strongly altered fragments with relict plagioclase and detrital quartz, altered to albite, adularia, quartz, illite, chlorite, epidote and rare apatite.

In the northeast injection area, samples from PK4A (1,395 mRF) are highly altered chlorite-rich fragments of siltstone of intermediate composition. Abundant chlorite is replacing the sedimentary cement and rare illite deposition is also noted. Figure 9 shows a framboidal pyrite (likely sedimentary) in a matrix of chlorite with quartz and rare titanite observed in PK4A sample. Cuttings from PK5 (2,465 mRF) are indicating poorly-sorted sandstone (Figure 10), with common fragments of chlorite-altered mafic to intermediate volcanic clasts. Quartz, plagioclase, epidote, chlorite and illite are common in the sample. Calcite is present in veins and as replacement mineral. Some of the chlorite-rich cuttings show siltstone to sheared / deformed greywacke texture (Figure 11). PK8 (core at 2,667 mRF), located just to the south of PK5, is showing well-sorted siltstone to sandstone fragments with common quartz, plagioclase and volcanic clasts in an illite + chlorite-rich matrix (Figure 12). The plagioclase clasts are heavily replaced by albite. The core is also crosscut by narrow veins of calcite (overprinted by chlorite and pyrite).

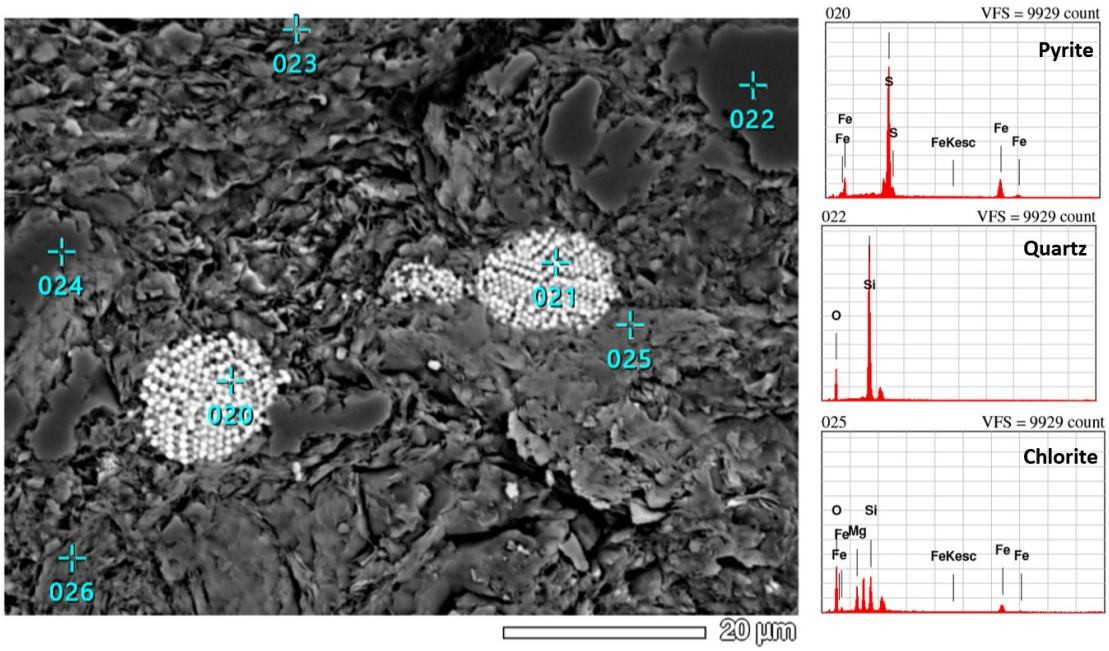


**Figure 9: PK4A-1395 mRF (left) framboidal pyrite (likely sedimentary) in a matrix of chlorite with quartz and rare titanite (Point 023). Right: EDS points mineral identification.**

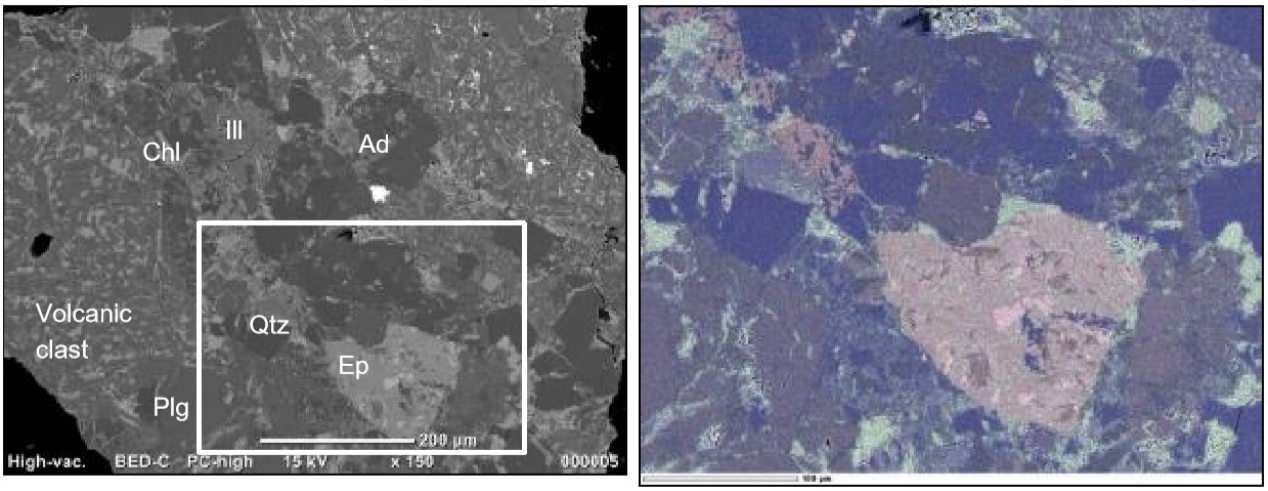


**Figure 10: PK5-2465 mRF (left) poorly-sorted sandstone, with fragments of chlorite-altered mafic to intermediate volcanic clasts. EDS chemical composite map (right) - red: Ca content, blue: Si content, green: Mg. (Legend: Ill-illite, Chl-chlorite, Ad-adularia, Qtz-quartz, Ep-epidote, Plg-plagioclase).**

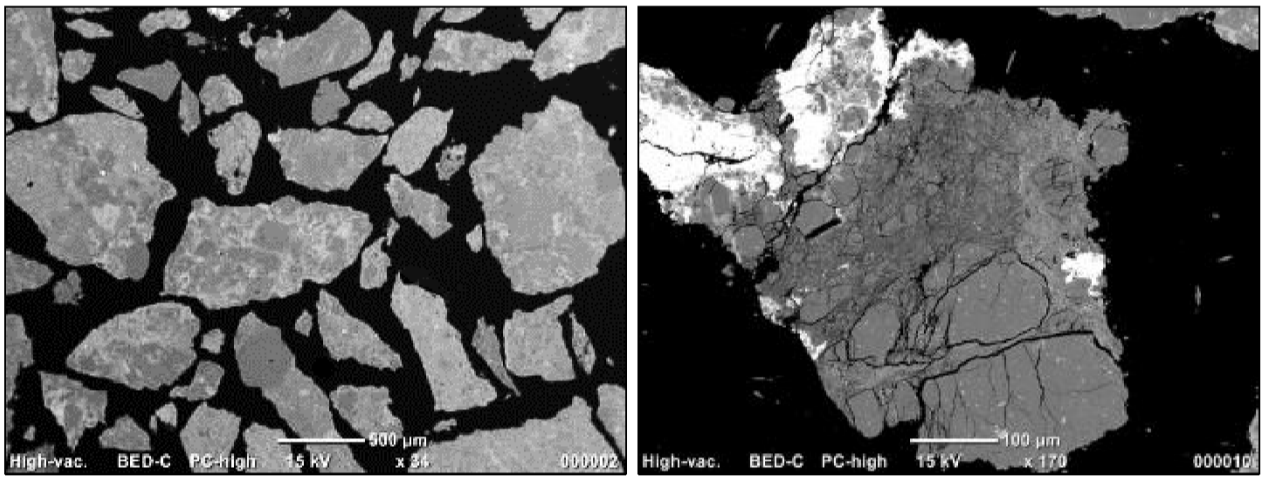


**Figure 11: PK5-2465 mRF. Chlorite-rich cuttings (left) composed of grains showing siltstone to deformed greywacke texture. Some fragments show intense pervasive calcite replacement. Right: Sheared and deformed fragments with pyrite mineralisation and cemented by chlorite and illite.**

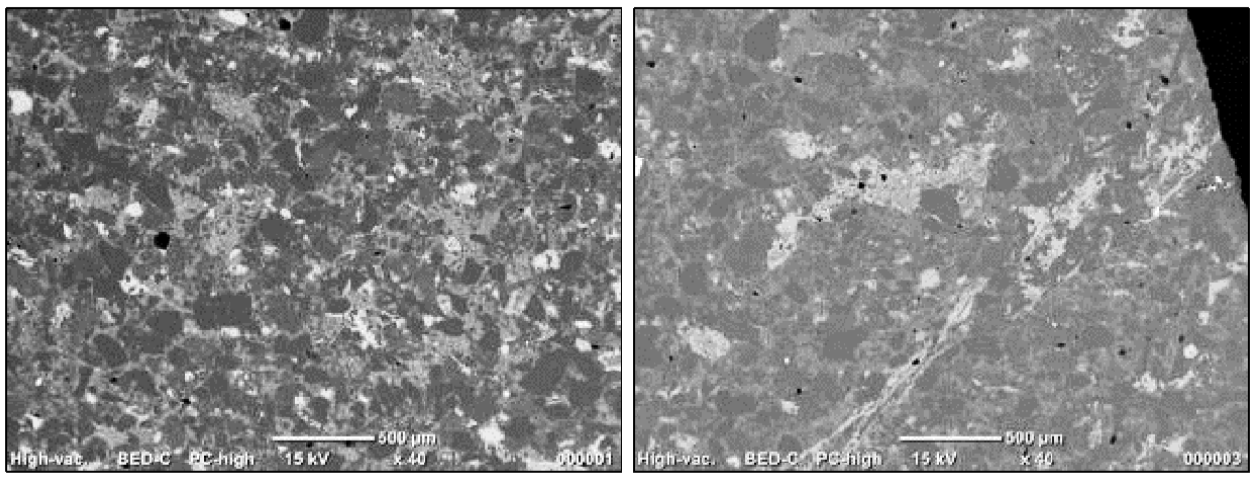


**Figure 12: PK8-2667 mRF (left) well-sorted siltstone / sandstone fragments with common quartz, plagioclase and volcanic clasts in an illite, chlorite-rich matrix. The core (right) is crosscut by narrow veins of calcite overprinted by chlorite and pyrite.**

### 5.2 Mineralogy

A summary of the minerals identified from the Rotokawa and Kawerau greywackes examined in this study is shown in Table 2. Calcite and epidote are both notably absent (i.e. below detection) in the Rotokawa greywacke while the Kawerau greywacke has 10 to 25 wt% calcite. The cuttings examined for KA55 (1580 mRF) and KA51 (1670 mRF) did not exhibit much calcite but further review of the overall greywacke package in those two wells suggest ~20 wt% calcite commonly occurring as vein-filling material. Figure 13 shows an example of a calcite vein observed in KA44 (2,000 mRF). Figure 14 (left) illustrates the large calcite grain seen in PK4A (1,495 mRF) and Figure 14 (right) highlights the pervasive calcite replacement in KA44 (2,000 mRF). Chlorite is also higher in the Kawerau greywacke (15 to 20 wt%) compared to the Rotokawa greywacke (5 to 15 wt%).

The Rotokawa greywacke is more illite-rich (20 to 40 wt% illite) than the Kawerau greywacke with 5 to 10 wt% illite. As shown in Figure 5 to Figure 8, illite is the main alteration mineral in the matrix of the sandstone / siltstone and in the fine-grained mudstones for the Rotokawa greywackes. Kawerau greywackes, in contrast, have less matrix and mostly metasandstone and siltstone.

Quartz, albite and adularia are also relatively higher in the Kawerau greywacke than in the Rotokawa greywacke which may reflect differences in the degree of alteration between the two greywackes.

**Table 2. Average % mineral abundance for selected Kawerau and Rotokawa greywacke samples.**

| Well | Depth, mRF* | Plagioclase | K-feldspar | Quartz | Calcite | Chlorite | Illite | Epidote | Albite | Adularia | Wairakite | TiOxide | Sulfide | Oxide-titanite | Oxide - Sulfide | Others |
|---|---|---|---|---|---|---|---|---|---|---|---|---|---|---|---|---|
| KA44 | 2000 | 8 | | 30 | 25 | 15 | 10 | | 8 | 3 | | 1 | | | | |
| KA51 | 1670 | 20 | 10 | 15 | | 15 | 10 | 5 | 15 | 5 | 5 | | 1 | | | |
| KA55 | 1580 | 10 | 5 | 25 | | 20 | 5 | 5 | 15 | 10 | | | | 5 | | Plus rare calcite, Fe oxide |
| PK4A | 1495 | 10 | 5 | 25 | 10 | 20 | 5 | 5 | 15 | | | | | | 5 | Plus rare titanite |
| PK5 | 2465 | 10 | 5 | 25 | 10 | 20 | 5 | 5 | 15 | | | | | | 5 | Plus rare titanite |
| PK8 | 1495 | 10 | 5 | 25 | 10 | 20 | 5 | 5 | 15 | | | | | | 5 | Plus rare titanite |
| RK4 | 2394 | 5 | 10 | 20 | <5 | 5 | 40 | <5 | 5 | | | | | | 5 | Plus rare titanite |
| RK20 | 2600 | 5 | 5 | 20 | <5 | 10 | 40 | <5 | 5 | | | | | | <5 | Plus rare titanite |
| RK21 | 2400 | 10 | 10 | 20 | <5 | 15 | 25 | <5 | 5 | | | | | | 5 | Plus rare titanite |
| RK22 | 2680 | 10 | 10 | 20 | <5 | 15 | 25 | <5 | 5 | | | | | | 5 | Plus rare titanite |
| RK23 | 2448 | 10 | 15 | 20 | <5 | 10 | 20 | <5 | 10 | | | | | | 5 | Plus rare titanite |
| RK24 | 2250 | 5 | 5 | 20 | <5 | 10 | 40 | <5 | 5 | | | | | | <5 | Plus rare titanite |

**mRF = measured depth in meters relative to Rig Floor*

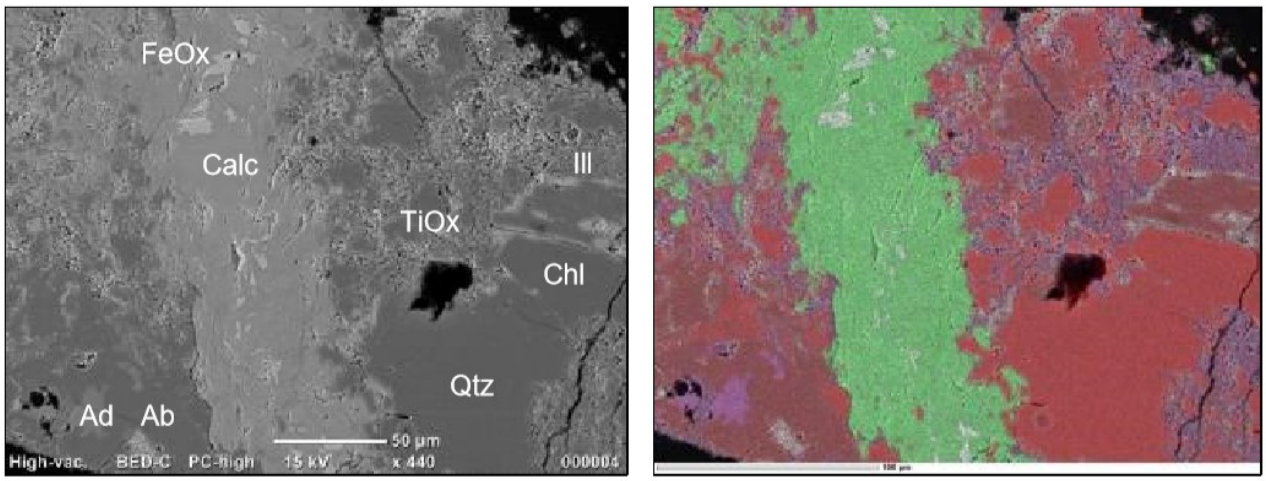


**Figure 13: KA44-2000 mRF (left) Example of a calcite vein. The hydrothermal alteration assemblage comprises quartz (Qtz), calcite (Calc), iron and titanium oxides (FeOx; TiOx), illite (Ill), chlorite (Chl), albite (Ab) and adularia (Ad). Right: EDS chemical composite map, red: $SiO_2$, violet: K (adularia, illite), green: Ca (calcite).**

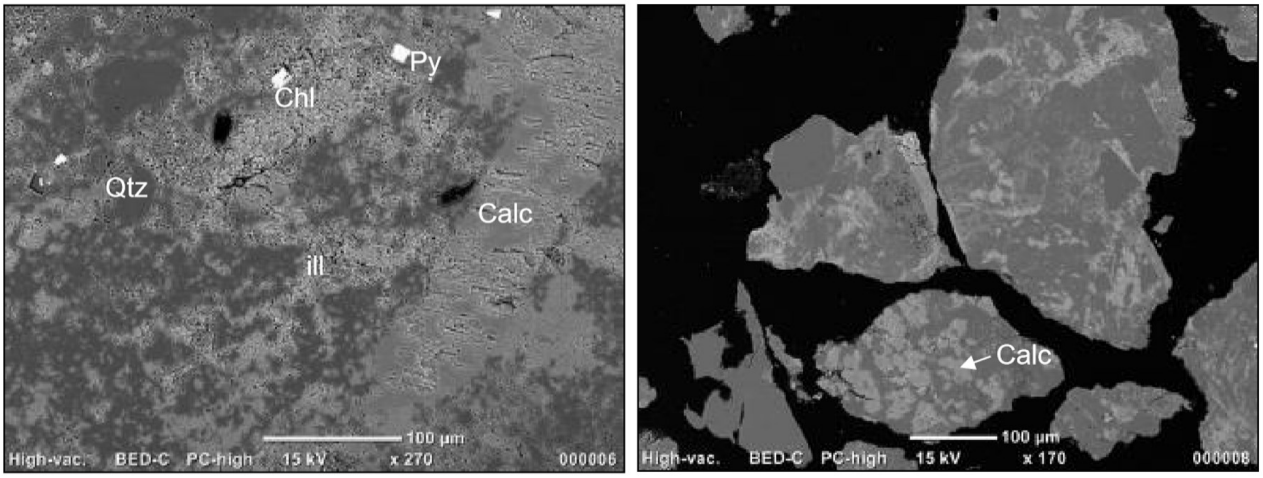


**Figure 14: PK4A-1395 mRF (left) large calcite grain (>200 mm long) with clasts composed of chlorite (Chl), quartz (Qtz), albitised plagioclase, and rare pyrite (Py) and illite (ill). Right: KA44-2000 mRF calcite-rich (Calc) fragments showing the pervasive nature of calcite replacement.**

### 5.3 Implication of mineralogy to greywacke reactivity

One key difference noted between the Rotokawa and Kawerau greywackes is the abundance of calcite occurring commonly as vein-material in the latter. As calcite reacts readily with acidic fluids, this may provide a pH-buffering effect that may have implication on the effectiveness of acid-dosing as silica scaling control for this type of host rock. Chlorite, which have similar buffering effect on pH, is also more abundant in the Kawerau greywacke. However, this finding does not discount other factors (such as temperature differences) that may contribute to the observed difference in injection well performance in the two fields.

## 5. CONCLUSIONS

Results of the petrographic and mineralogic review of selected Rotokawa and Kawerau greywacke basement reservoir rocks reveal differences in the two fields. Rotokawa greywacke varies from matrix-dominated, well-sorted metasandstone to argillite and characterized with abundant illite but rare to no calcite and epidote. Kawerau greywacke is instead generally well-sorted, clast-supported metasandstone to siltstone with common volcanic clasts of intermediate composition. Unlike Rotokawa, the Kawerau greywackes have high amounts of calcite (10-20 wt%) and chlorite (15-20 wt%). The abundance of these two minerals in the Kawerau greywacke is possibly influencing the rock reactivity to acid-dosed brine resulting to buffering of the fluid pH. This may help explain the observed difference in injection well performance between the two fields.

Based on petrographic characteristics, the samples from Rotokawa can be classified as part of the Torlesse Composite Terrane (Kaweka Terrane) while samples from Kawerau can be grouped under Waipapa Composite Terrane (Morrinsville Facies).

## 6. ACKNOWLEDGMENTS

The authors would like to acknowledge Mercury NZ Ltd. and Rotokawa Joint Venture Ltd. (RJV) for allowing us to publish this paper.

## 7. REFERENCES

Adams, C.J., Mortimer, N., Campbell, H.J., Griffin, W.L.: Age and Isotopic Characteristics of Metasedimentary Rocks from the Torlesse Supergroup and Waipapa Group in the Central North Island, New Zealand, *New Zealand Journal of Geology and Geophysics*, **52:2**, (2009), 149-170.

Askari, M., Azwar, L., Clark, J and Wong, C.: Injection Management in Kawerau Geothermal Field, New Zealand, *Proceedings*, World Geothermal Congress, Melbourne, Australia (2015).

Beetham, R.D., and Watters, W. A.: Geology of Torlesse and Waipapa terrane basement rocks encountered during the Tongariro Power Development project, North Island, New Zealand, *New Zealand Journal of Geology and Geophysics*, **28:4**, (1985), 575-594, DOI: 10.1080/00288306.1985.10422534.

Bloomer, A.: Kawerau Industrial Direct Use: Recent Developments, *Proceedings*, World Geothermal Congress, Melbourne, Australia (2015).

Cole, B., and Legmann, H.: The Rotokawa Geothermal Project: A High Pressure, Sustainable and Environmentally Benign Power Plant, Geothermal Resource Council Trans., 22, (1998).

Hernandez, D., Clearwater, J., Burnell, J., Franz, P., Azwar, L., and Marsh, A.: Update on the Modeling of the Rotokawa Geothermal System: 2010-2014, *Proceedings*, World Geothermal Congress, Melbourne, Australia (2015).

McNamara, D.D., Sewell, S., Buscarlet, E., and Wallis, I.C.: A Review of the Rotokawa Geothermal Field, New Zealand, *Geothermics*, **59**, (2016), 281-293, DOI: 10.1016/j.geothermics.2015.07.007.

Milicich, S.D., Clark, J.P., Wong, C and Askari, M.: A Review of the Kawerau Geothermal Field, New Zealand, *Geothermics*, **59**, (2015), 252-265, DOI: 10.1016/j.geothermics.2015.06.012.

Mortimer, N., Rattenbury, M.S., King, P.R., Bland, K.J., Barrell, D.J.A., Bache, F., Begg, J.G., Campbell, H.J., Cox, S.C., Crampton, J.S., Edbrooke, S.W., Forsyth, P.J., Johnston, M.R., Jongens, R., Lee, J.M., Leonard, G.S., Raine, J.I., Skinner, D.N.B., Timm, C., Townsend, D.B., Tulloch, A.J., Turnbull, R.E.: High-Level Stratigraphic Scheme for New Zealand Rocks, *New Zealand Journal of Geology and Geophysics*, **57:4**, (2014), 402-419, DOI: 10.1080/00288306.2014.946062.

New Zealand Geothermal Association: Historical Changes in NZ Geothermal Electricity Generation Capacity (2019), https://nzgeothermal.org.nz/geothermal-energy/electricity-generation/historical-changes-nz-geothermal-electricity-generation-capacity/

Price, R., Mortimer, N., Smith, IEM, and Maas, R.: Whole-Rock Geochemical Reference Data for Torlesse and Waipapa Terranes, North Island, New Zealand, *New Zealand Journal of Geology and Geophysics*, **58:3**, (2015), 1-16, DOI: 10.1080/00288306.2015.1026832.

Risk, G.F.: Electrical Resistivity of the Rotokawa Geothermal Field, New Zealand, *Proceedings,* 22nd New Zealand Geothermal Workshop, NZ (2000).

White, B.R., and Chambefort, I.: Geothermal development history of the Taupo Volcanic Zone, *Geothermics*, **59B**, (2016), 148-167.

Wood, C.P., Brathwaite, R., and Rosenberg, M.: Basement Structure, Lithology and Permeability at Kawerau and Ohaaki Geothermal Fields, New Zealand, *Geothermics*, **30**, (2001), 461-481, DOI:10.1016/S0375-6505(01)00003-7.